



OPEN

Irregular shape as an independent predictor of prognosis in patients with primary intracerebral hemorrhage

Chunyang Liu^{1,2,4}, Haopeng Zhang^{1,2,4}, Lixiang Wang^{1,2,4}, Qiuyi Jiang^{1,2}, Enzhou Lu^{1,2}, Chao Yuan^{1,2}, Yanchao Liang^{1,2}, Zhenying Sun^{1,2}, Huan Xiang^{1,2}, Xun Xu^{1,2}, Jingxian Sun^{1,2}, Bo Fu³, Boxian Zhao^{1,2}, Daming Zhang^{1,2}, Xin Chen^{1,2}, Ning Wang^{1,2}✉, Lu Wang³✉ & Guang Yang^{1,2}✉

The utility of noncontrast computed tomography markers in the prognosis of spontaneous intracerebral hemorrhage has been studied. This study aimed to investigate the predictive value of the computed tomography (CT) irregularity shape for poor functional outcomes in patients with spontaneous intracerebral hemorrhage. We retrospectively reviewed all 782 patients with intracranial hemorrhage in our stroke emergency center from January 2018 to September 2019. Laboratory examination and CT examination were performed within 24 h of admission. After three months, the patient's functional outcome was assessed using the modified Rankin Scale. Multinomial logistic regression analyses were applied to identify independent predictors of functional outcome in patients with intracerebral hemorrhage. Out of the 627 patients included in this study, those with irregular shapes on CT imaging had a higher proportion of poor outcomes and mortality 90 days after discharge ($P < 0.001$). Irregular shapes were found to be significant independent predictors of poor outcome and mortality on multiple logistic regression analysis. In addition, the increase in plasma D-dimer was associated with the occurrence of irregular shapes ($P = 0.0387$). Patients with irregular shapes showed worse functional outcomes after intracerebral hemorrhage. The elevated expression level of plasma D-dimers may be directly related to the formation of irregular shapes.

Abbreviations

| | |
|------|----------------------------------|
| CI | Confidence interval |
| CT | Computed tomography |
| CTA | Computed tomography angiography |
| GCSs | Glasgow Coma Scale score |
| HE | Hematoma expansion |
| ICH | Intracerebral hemorrhage |
| IQR | Interquartile range |
| mRS | Modified Rankin Scale |
| NCCT | Non-contrast computed tomography |
| OR | Odds ratio |
| OS | Overall survival |
| SD | Standard deviation |

Spontaneous intracranial hemorrhage (ICH), a subtype of stroke with a severe high mortality and disability rate, accounts for approximately 10–15% of all stroke patients^{1–3}. Early hematoma expansion (HE), frequently

¹Department of Neurosurgery, The First Affiliated Hospital of Harbin Medical University, Youzheng Street 23, Nangang District, Harbin 150001, Heilongjiang Province, China. ²Institute of Brain Science, Harbin Medical University, Harbin, China. ³Department of Urology, The Fourth Hospital of Harbin Medical University, Yiyuan Street 37, Nangang District, Harbin 150001, Heilongjiang Province, China. ⁴These authors contributed equally: Chunyang Liu, Haopeng Zhang and Lixiang Wang. ✉email: wangningprofessor@163.com; wanglukaixin360@163.com; yangguang@hrbmu.edu.cn

accompanied by the occurrence of neurological deterioration, is associated with poor functional outcomes in patients with intracerebral hemorrhage⁴. The heterogeneity of hematoma has been verified to be associated with hematoma expansion^{5,6}. Although the CT angiography (CTA) spot sign is accepted as the gold standard for judging the risk of hematoma expansion⁷, the need for a contrast agent limits its availability and poses an additional risk for some patients. Therefore, the prompt and accurate identification of patients that at high risk of developing hematoma expansion and giving them individualized treatment measures may provide benefits in functional outcomes^{8,9}. Compared with CTA, noncontrast computed tomography (NCCT) is an inexpensive and widely used examination tool that is more suitable for early diagnostic applications in patients with intracerebral hemorrhage¹⁰. Some NCCT biomarkers of intracerebral hemorrhage have received increasing attention from researchers for their good performance in predicting the poor prognosis of patients. Morotti et al. showed good predictive performance when the irregular shape was used as an NCCT marker for judging early intracerebral hemorrhage expansion¹¹. However, this study was based on unadjusted pooled estimates, there was no independent collection of real patient medical records for analysis, and the factors associated with the appearance of irregular shapes have not been explored.

Therefore, in this study, we comprehensively collected the clinical data of patients with intracerebral hemorrhage and explored whether the irregular shape could serve as an independent predictor for judging patient prognosis. In our previous studies, it was confirmed that plasma D-dimer expression levels can predict the poor prognosis of patients with intracerebral hemorrhage¹². On this basis, we further investigated whether there was a specific correlation between the appearance of the irregular shape of the hematoma and the elevated expression level of plasma D-dimer.

Patients and methods

Patients. The clinical data of 782 patients with ICH admitted to the emergency neurosurgery ward of the First Affiliated Hospital of Harbin Medical University from January 2018 to September 2019 were retrospectively analyzed. The inclusion and exclusion criteria were as follows: age ≥ 18 years; CT scans performed within 24 h of admission; and standard techniques used (CA-7000 Sysmex; Dade Behring) to analyze the concentration of D-dimer. Patients without CT images or follow-up CT scans within 24 h after the initial CT examination, patients with intracranial hemorrhage due to trauma or aneurysm, and patients with infratentorial hemorrhage were excluded.

To assess the clinical status, the Glasgow Coma Scale (GCS) score was measured by a neurosurgeon at the time of patient admission. To determine the functional outcome, patients were followed up at least three months after symptom onset, and their clinical outcomes were assessed by the modified Rankin scale (mRS; poor functional outcome: mRS score 4–6; favorable functional outcome: mRS score 0–3). In addition, all patients were followed for survival status until death or the end of the study. The last date of Study period (September 30, 2020) was used as an end date. The study protocol was approved by the Institutional Review Board of The First Affiliated Hospital of Harbin Medical University. Simultaneously, all methods were carried out in accordance with the relevant regulations and guidelines of Harbin Medical University.

Image features. The imaging data of the patients were evaluated independently by two experienced neurologists. Hematoma volumes were measured on industry-standard DICOM images using 3D Slicer 4.10.2, an open-source software (SPL, Harvard Medical School, Boston, USA). For patients with severe symptoms, continuous deterioration, and suspected intracerebral hemorrhage expansion, the noncontrast CT scans will be examined within 24 h after admission, and the presence of hematoma expansion and irregular shapes will be judged. Hematoma expansion was defined as an absolute growth > 6 mL or a relative growth $> 33\%$ in hematoma size on follow-up nonenhanced CT scans compared with the initial CT examination after admission¹³. Irregular shapes were defined as the presence of two or more connected or separated irregular hematomas at the edge of the hematoma on the axial section with the largest hematoma cross-sectional area¹⁴ (Supplemental Fig. 1).

Statistical analysis. Statistical analysis and calculations were carried out using dedicated software (IBM SPSS Statistics 21.0; SPSS Inc, Armonk, NY, USA) or GraphPad Prism 8 software (version 8.0.3; GraphPad Software Inc, San Diego, CA). Baseline characteristics were compared between patients with and without hematoma expansion. Categorized variables were expressed as counts (percentages) and compared using the chi-square test or Fisher's exact test, while continuous variables were expressed as the mean \pm SD or median (interquartile range, IQR) values and compared using independent sample Student's *t* test.

Variables associated with mortality at 90 days after discharge, poor prognosis, and hematoma enlargement were included in the univariate analysis. Variables with *P* values < 0.05 in the univariate analysis were included in multivariate logistic models to adjust for confounders. The scatter plot represents the relationship between irregular shape and plasma D-dimer expression levels. Statistical significance for all tests was defined as $P < 0.05$.

Consent to participate. The need for informed consent was waived due to the retrospective nature of the study.

Consent for publication. The need for informed consent was waived due to the retrospective nature of the study. The manuscript does not contain identifying details.

Ethical approval. The study protocol was approved by the Institutional Review Board of The First Affiliated Hospital of Harbin Medical University. Simultaneously, all methods were carried out in accordance with the rel-

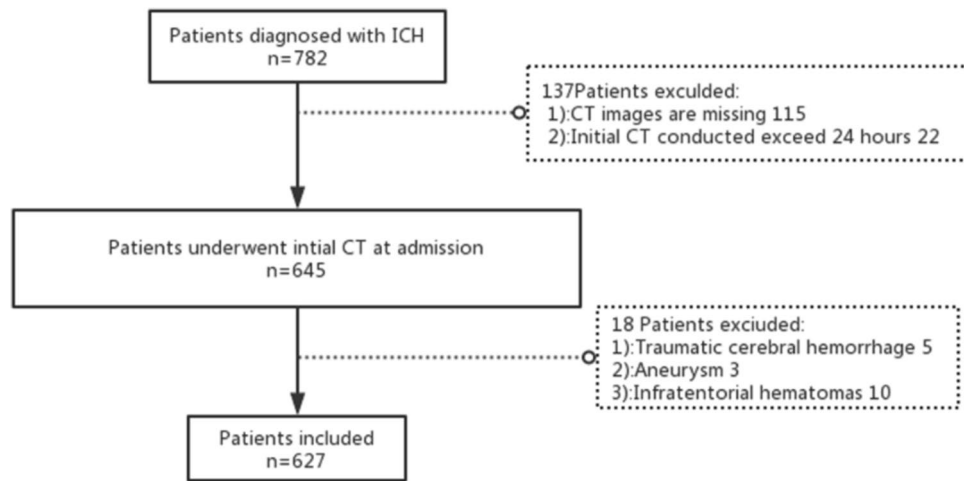


Figure 1. Flowchart of patient enrollment.

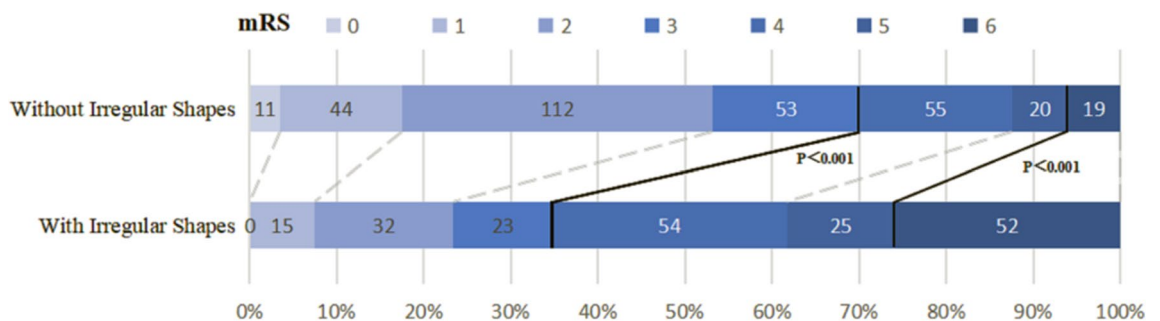


Figure 2. Distribution of the modified Rankin Scale (mRS) scores according to the presence or absence of irregular shapes. The bold line separates favorable (mRS, 0–3) and poor outcomes (mRS, 4–6) or survival and death.

evant regulations and guidelines of Harbin Medical University. And has therefore been performed in accordance with the ethical standards laid down in the 1964 Declaration of Helsinki and its later amendments. The need for informed consent was waived by the Institutional Review Board of The First Affiliated Hospital of Harbin Medical University due to the retrospective nature of the study.

Results

According to the inclusion and exclusion criteria, 782 patients were included in our study. Figure 1 shows the study flow chart of patient inclusion for the analysis. There were 627 eligible patients, including 428 males and 199 females. The mean age of the patients was 57.95 years (range 18–91 years). The mean hematoma volume of all patients was 25.56 ± 27.91 mL, the mean plasma D-dimer level on admission was 1.36 ± 4.69 mg/L, and a total of 220 patients had an elevated expression level of D-dimer on admission (35.0%). Hematoma expansion was observed in 43 patients, 28 of whom presented with irregular shapes. Among the 627 patients included in this study, 248 were diagnosed with irregular shapes. The 515 patients in the study were able to continue our follow-up investigation 90 days after discharge. In patients with irregular shapes, there was a significantly higher rate of poor outcomes and mortality at 90 days after discharge (mRS = 4–6 at 3 months: positive 131/201 [65.1%] vs. negative 94/314 [29.9%], $P < 0.001$; mortality at 3 months: positive 52/201 [25.9%] vs. negative 19/314 [6.1%], $P < 0.001$; Fig. 2). Table 1 shows the comparison of clinical characteristics between patients with irregular shapes and the control group. The results showed that initial blood pressure, initial hematoma volume, hematoma expansion, presence of IVH, degree of midline shift, and elevated plasma D-dimer levels were significantly related to the occurrence of irregular shapes.

Univariate logistic regression analysis was performed for poor outcome and mortality after 90 days of discharge in patients with ICH, and the factors associated with the development of hematoma expansion within 24 h of admission were explored (Table 2). The analysis results indicated a significantly higher rate of early hematoma expansion in patients with irregular shapes (OR = 3.776, 95% CI 1.950–7.312, $P < 0.001$) and had a poor prognosis at 90 days (OR = 4.380, 95% CI 3.003–6.389, $P < 0.001$) and an expressively higher mortality rate (OR = 5.233, 95% CI 2.991–9.155, $P < 0.001$). The results also indicated that patients with elevated plasma D-dimer levels had a higher risk of mortality (OR = 3.518, 95% CI 2.096–5.905, $P < 0.001$) and poorer prognosis (OR = 2.809, 95% CI 1.928–4.092, $P < 0.001$). Multivariate logistic regression analyses were performed for significant variables in the

| Characteristics | Patients, no. (%) | | P value |
|------------------------------------|--|---|---------|
| | Patients with irregular sign (n = 248) | Patients without irregular sign (n = 379) | |
| Age (years) | 57.82 ± 11.57 | 58.04 ± 11.48 | 0.812 |
| Sex (male) | 165 (66.5) | 263 (69.4) | 0.452 |
| History of hypertension | 230 (92.7) | 342 (90.5) | 0.323 |
| History of diabetes | 29 (11.7) | 40 (10.6) | 0.664 |
| First systolic BP (mmHg) | 176.88 ± 29.73 | 168.33 ± 26.55 | <0.001 |
| Heart rate | 79.54 ± 19.71 | 80.25 ± 16.58 | 0.643 |
| Temperature (°C) | 36.60 ± 0.33 | 36.57 ± 0.24 | 0.198 |
| Initial hematoma volume (ml) | 27.95 (15.03–51.84) | 9.98 (4.16–23.05) | <0.001 |
| Hematoma expansion | 28 (17.5) | 15 (5.3) | <0.001 |
| IVH | 107 (43.1) | 115 (30.3) | 0.001 |
| Location of ICH | | | 0.733 |
| Lobar | 25 (10.1) | 35 (9.2) | |
| Deep | 223 (89.9) | 344 (90.8) | |
| Midline shift (mm) | 5.14 (4.57–5.70) | 2.19 (1.87–2.50) | <0.001 |
| Admission INR | 1.01 (0.99–1.03) | 1.01 (0.99–1.03) | 0.965 |
| Admission PT (s) | 11.10 (10.60–11.80) | 11.20 (10.80–11.70) | 0.896 |
| Admission APTT (s) | 25.60 (23.70–27.80) | 25.75 (23.90–27.70) | 0.683 |
| Admission Fibrinogen (g/L) | 2.85 (2.73–2.97) | 2.96 (2.76–3.16) | 0.417 |
| Admission D-Dimer, > 0.55 mg/L FEU | 103 (41.7) | 117 (31.5) | 0.009 |
| GCS score on admission | 11.01 ± 2.74 | 11.41 ± 2.57 | 0.063 |
| Surgery | 103 (41.5) | 77 (20.3) | <0.001 |

Table 1. Clinical characteristics related to Irregular Sign in patients with ICH. APTT = activated partial thromboplastin time, BP = blood pressure; GCS = Glasgow Coma Scale; ICH = intracerebral hemorrhage; INR = international normalized ratio; IVH = intraventricular hemorrhage on presentation; mRS = modified Rankin Scale; NIHSS = NIH Stroke Scale; PT = prothrombin time. Values are n (%), mean ± SD, or median (interquartile range).

| Variable | 90-day poor outcome | | | 90-day mortality | | | HE | | |
|------------------------------------|---------------------|-------------|---------|------------------|-------------|---------|-------|--------------|---------|
| | OR | 95% CI | P value | OR | 95% CI | P value | OR | 95% CI | P value |
| Age (years) | 1.037 | 1.020–1.054 | <0.001 | 1.032 | 1.009–1.055 | 0.006 | 0.984 | 0.957–1.012 | 0.261 |
| Sex (male) | 0.988 | 0.678–1.438 | 0.948 | 0.975 | 0.568–1.673 | 0.926 | 0.352 | 0.153–0.811 | 0.014 |
| History of hypertension | 1.608 | 0.843–3.067 | 0.150 | 1.675 | 0.582–4.823 | 0.339 | 1.322 | 0.390–4.489 | 0.654 |
| History of diabetes | 1.229 | 0.698–2.161 | 0.475 | 1.196 | 0.560–2.553 | 0.643 | 0.940 | 0.353–2.502 | 0.901 |
| First systolic BP (mmHg) | 1.016 | 1.009–1.022 | <0.001 | 1.025 | 1.015–1.034 | <0.001 | 1.009 | 0.998–1.021 | 0.100 |
| Heart rate | 1.012 | 1.002–1.023 | 0.021 | 1.024 | 1.011–1.038 | <0.001 | 0.991 | 0.971–1.011 | 0.373 |
| Temperature | 1.769 | 0.915–3.421 | 0.090 | 2.120 | 0.906–4.962 | 0.083 | 0.657 | 0.179–2.412 | 0.527 |
| Initial hematoma volume (mL) | 1.043 | 1.033–1.054 | <0.001 | 1.039 | 1.029–1.048 | <0.001 | 1.025 | 1.012–1.038 | <0.001 |
| IVH | 3.283 | 2.258–4.772 | <0.001 | 3.576 | 2.125–6.018 | <0.001 | 1.071 | 0.547–2.097 | 0.842 |
| Location of ICH | 1.355 | 0.757–2.425 | 0.307 | 0.577 | 0.283–1.178 | 0.131 | 0.800 | 0.297–2.154 | 0.659 |
| Midline shift | 1.258 | 1.189–1.332 | <0.001 | 1.260 | 1.186–1.339 | <0.001 | 1.140 | 1.046–1.243 | 0.003 |
| Admission INR | 1.365 | 0.567–3.290 | 0.488 | 1.646 | 0.640–4.234 | 0.301 | 1.109 | 0.271–4.531 | 0.886 |
| Admission PT (s) | 1.036 | 0.950–1.131 | 0.423 | 1.059 | 0.966–1.160 | 0.221 | 0.999 | 0.858–1.162 | 0.985 |
| Admission APTT, s | 0.912 | 0.863–0.965 | 0.001 | 0.972 | 0.901–1.048 | 0.461 | 1.016 | 0.927–1.114 | 0.731 |
| Admission D-Dimer, > 0.55 mg/L FEU | 2.809 | 1.928–4.092 | <0.001 | 3.518 | 2.096–5.905 | <0.001 | 1.032 | 0.533–1.998 | 0.926 |
| Admission fibrinogen (g/L) | 1.062 | 0.949–1.188 | 0.294 | 0.969 | 0.721–1.154 | 0.721 | 0.626 | 0.413–0.949 | 0.027 |
| Irregular sign | 4.380 | 3.003–6.389 | <0.001 | 5.233 | 2.991–9.155 | <0.001 | 3.776 | 1.950–7.312 | <0.001 |
| GCS score on admission | 0.900 | 0.842–0.962 | 0.002 | 0.862 | 0.790–0.940 | 0.001 | 0.958 | 0.851–1.078 | 0.474 |
| Surgery | 3.054 | 2.060–4.527 | <0.001 | 0.668 | 0.396–1.129 | 0.132 | 7.674 | 3.941–14.942 | <0.001 |

Table 2. Univariate associations with poor functional outcomes (mRS 3–6) and mortality and hematoma expansion. APTT = activated partial thromboplastin time, BP = blood pressure; CI = confidence interval; GCS = Glasgow Coma Scale; ICH = intracerebral hemorrhage; INR = international normalized ratio; IVH = intraventricular hemorrhage on presentation; mRS = modified Rankin Scale; NIHSS = NIH Stroke Scale; PT = prothrombin time. Values are n (%), mean ± SD, or median (interquartile range).

| Variable | 90-day poor outcome | | | 90-day mortality | | | HE | | |
|------------------------------|---------------------|-------------|---------|------------------|-------------|---------|-------------|-------------|---------|
| | Adjusted OR | 95% CI | P value | Adjusted OR | 95% CI | P value | Adjusted OR | 95% CI | P value |
| Age (years) | 1.052 | 1.031–1.074 | < 0.001 | 1.034 | 1.004–1.065 | 0.026 | 0.978 | 0.947–1.011 | 0.188 |
| First systolic BP (mmHg) | 1.009 | 1.000–1.017 | 0.045 | 1.014 | 1.002–1.025 | 0.019 | 1.008 | 0.996–1.020 | 0.211 |
| Heart rate | 1.012 | 0.998–1.027 | 0.095 | 1.021 | 1.004–1.037 | 0.014 | 0.990 | 0.969–1.012 | 0.375 |
| Irregular sign | 3.216 | 2.023–5.112 | < 0.001 | 2.689 | 1.376–5.255 | 0.004 | 2.527 | 1.211–5.275 | 0.014 |
| Midline shift | 1.070 | 0.982–1.165 | 0.121 | 1.041 | 0.944–1.147 | 0.421 | 1.007 | 0.878–1.155 | 0.923 |
| Initial hematoma volume (mL) | 1.040 | 1.010–1.040 | 0.001 | 1.023 | 1.009–1.038 | 0.002 | 1.020 | 1.000–1.041 | 0.048 |
| D-dimer, > 0.55 mg/L FEU | 1.367 | 0.830–2.252 | 0.219 | 1.548 | 0.767–3.124 | 0.223 | 1.209 | 0.540–2.706 | 0.644 |
| Admission APTT (s) | 0.975 | 0.911–1.044 | 0.467 | 1.098 | 1.007–1.199 | 0.035 | 1.048 | 0.946–1.160 | 0.370 |
| Admission fibrinogen (g/L) | 1.056 | 0.939–1.188 | 0.363 | 0.791 | 0.563–1.110 | 0.175 | 0.612 | 0.391–0.957 | 0.031 |
| GCS score on admission | 0.935 | 0.862–1.014 | 0.103 | 0.869 | 0.781–0.967 | 0.010 | 0.989 | 0.871–1.122 | 0.860 |
| IVH | 2.002 | 1.257–3.189 | 0.003 | 1.874 | 0.961–3.653 | 0.065 | 0.806 | 0.372–1.744 | 0.583 |

Table 3. Multiple associations with Poor Functional Outcome (mRS 3–6) and Mortality and Hematoma expansion. BP = blood pressure; CI = confidence interval; GCS = Glasgow Coma Scale; ICH = intracerebral hemorrhage; IVH = intraventricular hemorrhage on presentation; mRS = modified Rankin Scale. Values are n (%), mean \pm SD, or median (interquartile range).

univariate logistic analysis. Multivariate regression analysis showed that age (OR = 1.052, 95% CI 1.031–1.074, $P < 0.001$), first systolic blood pressure (OR = 1.008, 95% CI 1.001–1.017, $P = 0.049$), irregular shapes (OR = 3.190, 95% CI 2.007–5.070, $P < 0.001$), initial hematoma volume (OR = 1.024, 95% CI 1.009–1.039, $P = 0.001$), and intraventricular hemorrhage upon presentation (OR = 1.967, 95% CI 1.237–3.128, $P = 0.004$) independently predicted poor outcome of ICH. The irregular shape had equally good performance in independently predicting mortality (OR = 2.744, 95% CI 1.415–5.321, $P = 0.003$) and early hematoma expansion (OR = 2.607, 95% CI 1.711–3.974, $P < 0.001$) in patients with spontaneous intracerebral hemorrhage (Table 3). To explore whether the performance of different NCCT imaging markers in predicting poor prognosis of patients with intracerebral hemorrhage is superior to the irregular shape, we comprehensively interpreted the NCCT imaging markers, including the Island sign and Blend sign, in 627 spontaneous ICH patients included in our study. The predictive performance of different NCCT imaging markers for poor outcomes in ICH patients was analyzed with specificity and sensitivity, and the ROC curve was drawn. Our results demonstrated that irregular shape was better than other NCCT imaging markers for predicting the occurrence of unfavorable outcomes in ICH patients (area under the curve-AUC = 0.819, sensitivity 74.0%, specificity 78.7%, CI 0.781–0.856, Fig. 3A–C). Furthermore, in our study, the appearance of irregular shapes of the hematoma was a better predictor of poor patient functional outcome than the initial hematoma volume. (AUC = 0.808, Fig. 3D).

All patients will be followed up until death or the end of the study. A total of 535 patients were included in the Kaplan–Meier survival analysis, except for 92 patients whose death information was missing. The longest follow-up among all patients reached 32 months, with a median of 20 months, and by the end of the study on September 30, 2020 (Fig. 4). The results showed that the irregular shape of the hematoma was significantly associated with shorter survival of patients with cerebral hemorrhage ($P < 0.001$). In addition, in the data analysis, we also found that the appearance of irregular shapes was accompanied by altered plasma D-dimer expression levels, so we speculated whether the generation of irregular shapes resulted from the increased plasma D-dimer expression. In the scatter plot, plasma D-dimer expression levels were significantly correlated with the appearance of irregular shapes ($P = 0.039$, Fig. 5).

Discussion

Our statistical results shows that irregular shape has predictive significance for the prognosis of patients with ICH. Though island sign, blend sign and initial hematoma volume also have some prognostic value for ICH, the predictive value of irregular shape for the prognosis of ICH is still more significant comparing with them.

As a severely disabling neurological disease, spontaneous intracerebral hemorrhage (ICH) is receiving more and more attention on how to quickly and accurately predict the occurrence of its adverse consequences, and then help clinicians to grade and manage patients. Regarding imaging, although there remain some controversies surrounding the clear definition and formation mechanism of the spot sign on CTA, it has been recognized as a well-established imaging marker with 51%–91% sensitivity and 58%–89% specificity for predicting the occurrence of hematoma expansion in the short term in ICH patients^{7,15}, and the spot sign has also been identified as an independent predictor of poor prognosis in intracerebral hemorrhage. However, the need for contrast media for some patients (e.g., kidney failure, contrast allergy) limits CTA availability. The extravasation of contrast medium that occurs during CTA procedures may contribute to the occurrence of rebleeding¹⁶, posing an additional risk for some patients, which is not routinely performed in emergencies. Therefore, researchers have gradually explored the predictive value of NCCT markers, including the blend sign, irregular shape, and island

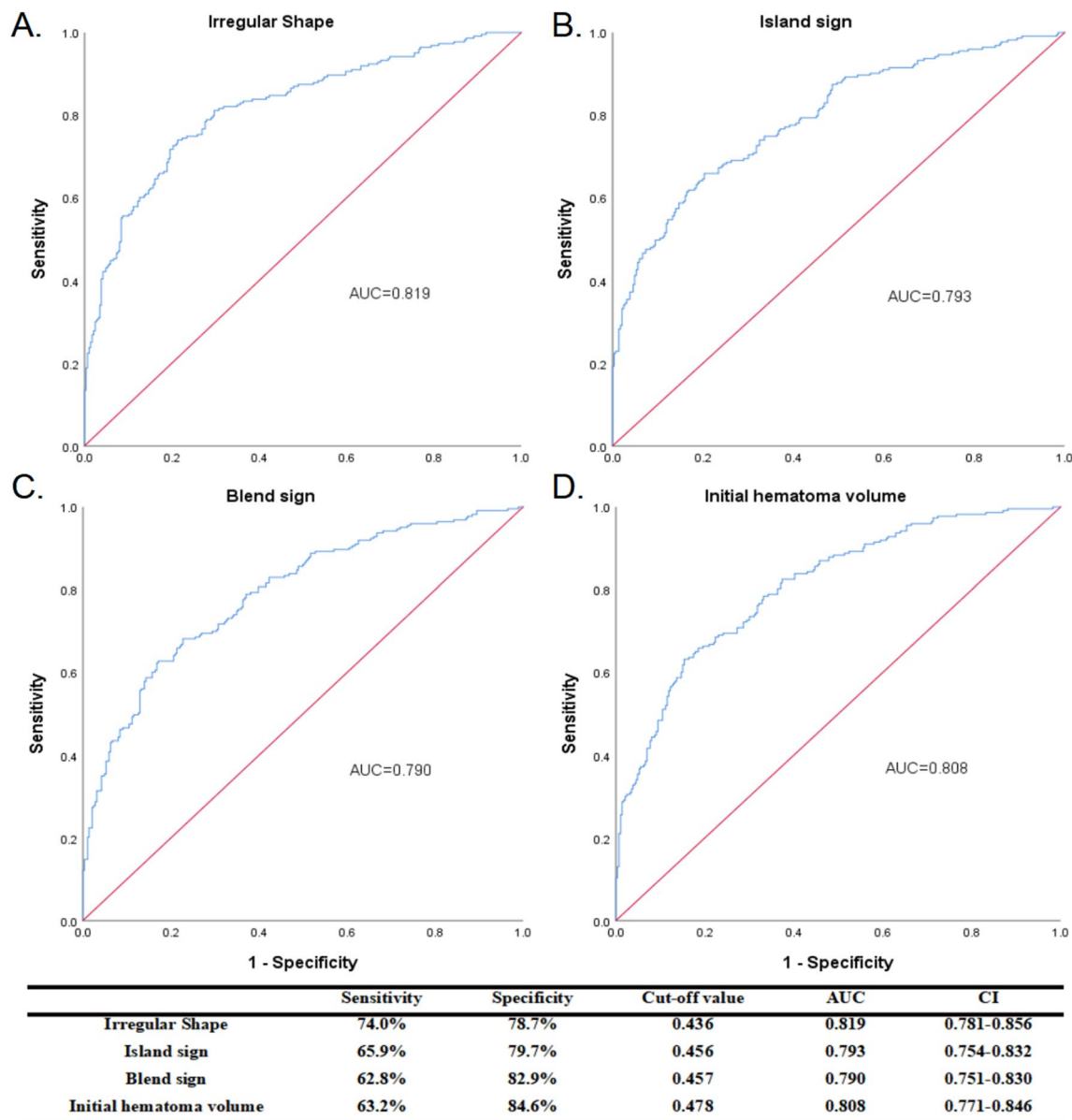


Figure 3. Receiver operating characteristic curves of irregular shape, island sign, blend sign, and IHV with their corresponding areas under the curve (AUCs) for predicting poor prognosis. The best cut-off points were identified with their sensitivity, specificity, and confidence interval (CI), respectively.

sign, for intracerebral hemorrhage expansion, and the results showed equally good predictive performance^{11,17}. Qi et al., in a retrospective analysis of 252 patients with intracerebral hemorrhage, showed that the island sign was an independent predictor of hematoma enlargement and poor outcomes in patients with ICH¹⁸. In a study conducted by Zhang et al. 1111 patients with ICH were recruited, and it was found that blend signs could help doctors grade the management of patients with intracerebral hemorrhage at admission¹⁹. In this study, we also analyzed the performance of different NCCT image markers in predicting poor functional prognosis in patients with cerebral hemorrhage, and the results showed good performance. In which the predictive power of irregular shapes was the best. In addition, many studies have demonstrated the significant value of hematoma volume for the prediction of prognostic situations in patients with intracerebral hemorrhage^{20–23}. In our study, initial hematoma volume predicted poor functional outcomes in patients than irregularly shaped hematomas.

In a previous study, Moratti et al. established a scoring system to predict the instability of the hematoma based on three indicators: presence or absence of the mixed sign, time to the appearance of the mixed sign, and reduction in the density of the hematoma at presentation²⁴. However, these studies did not directly use the irregular shape of the hematoma to evaluate the prognosis of patients and did not explore the cause of NCCT imaging hallmarks.

The overall survival (OS) of patients with irregular shapes in our study was significantly shorter than that of patients without irregular shapes. During a follow-up of up to 32 months for all patients included in this study,

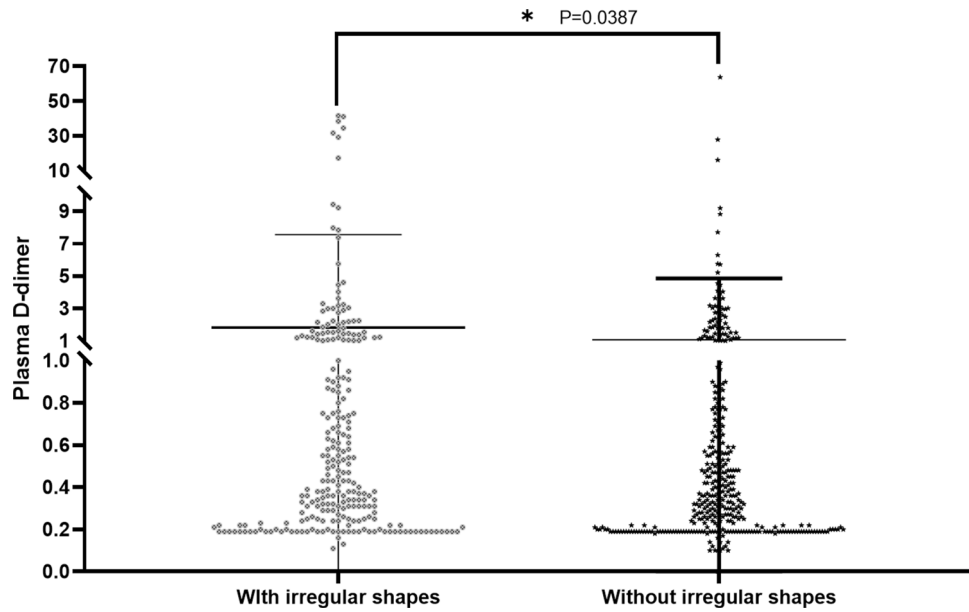


Figure 4. Kaplan–Meier curve analysis showing that the overall survival of patients with spontaneous intracerebral hemorrhage with irregular shapes in intracranial hematoma as worse than that with stable hematoma.

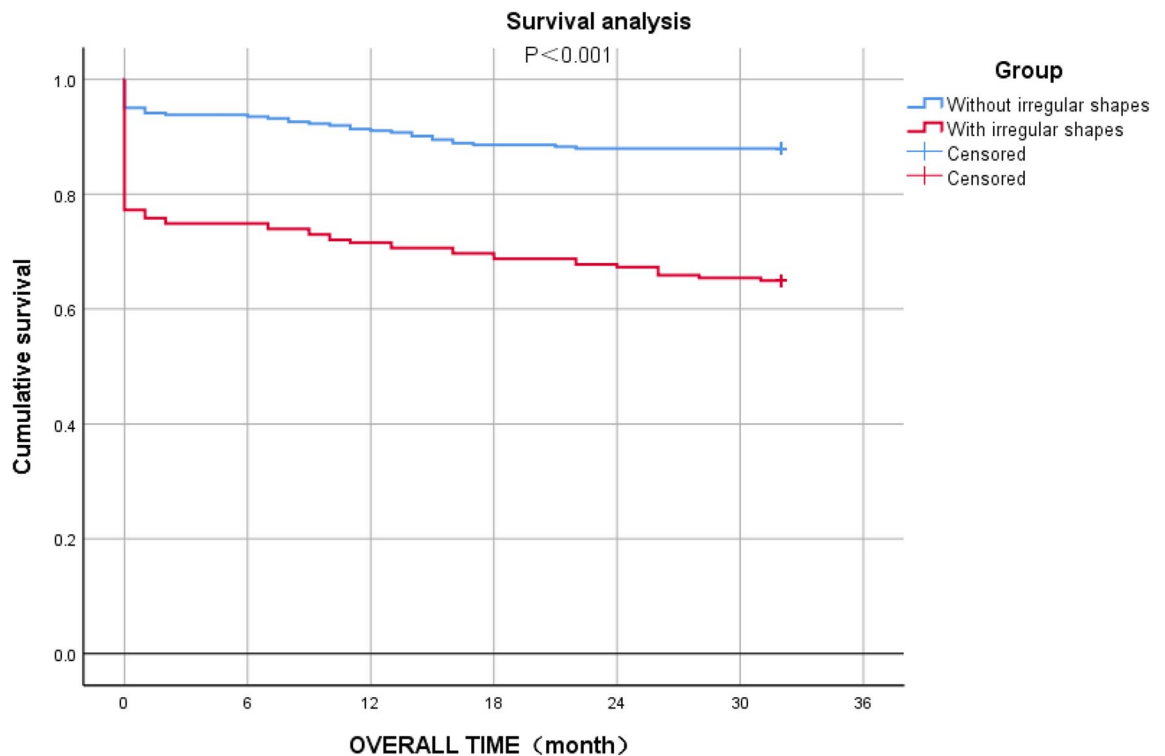


Figure 5. Scatter plot showing the relationship between the irregular shape and plasma D-dimer expression level. The appearance of irregular shapes in patients is often accompanied by an increase in plasma D-dimer expression on admission.

we recorded in detail the survival performance as well as the functional outcome status (mRS score) of patients with intracerebral hemorrhage after discharge. To our knowledge, this is the study with the longest follow-up time for a large number of patients among the relevant studies. Although we found death information for 20 of these patients by asking community hospitals or inquiring about patient death records, the survival status of 92 patients with ICH after discharge was unavailable.

The reason for the formation of irregular shape imaging signs was not deeply investigated in a large number of previous studies. In the present study, we showed for the first time that the appearance of irregular shapes was significantly associated with the elevation of plasma D-dimer (> 0.55 mg/L FEU). Plasma D-dimer has been shown to have good performance in the prediction of poor outcomes and mortality in patients with spontaneous ICH^{12,25,26}. Acute brain injury resulting from hematoma formation is closely related to coagulation activation, while D-dimer, the final product of coagulation, is a fibrin degradation product released from plasmin degrading fibrin monomers²⁷, and its expression quantity reflects the activation level of the systemic coagulation response. The massive release of thrombin, which induces inflammatory reactions in the perivascular tissues and then damages the blood–brain barrier (BBB), may lead to early hematoma expansion^{28,29}. However, there was no significant statistical association between plasma D-dimer levels and hematoma expansion at admission in this study, which may be related to sample size and systematic error.

Our study has certain limitations. First, the patients included in this study were all hospitalized in the stroke emergency center of our hospital. Although other hospitals in the city have also established stroke centers, they are small and have low comprehensive diagnosis and treatment capacity, so patients with severe disease will more likely be treated in our hospital. This may contribute to a worse functional prognosis and even higher mortality in the patient population included in this study.

Second, some patients may have delayed going to the hospital for treatment, so the delay in time from symptom onset to admission and CT scans may have affected some variables in this study, for example, hematoma expansion, as they may have stabilized before the first CT examination. Previous studies have demonstrated that hematoma expansion is more likely to occur within the first hour of intracerebral hemorrhage symptom onset³⁰. However, it is very difficult to obtain a precise judgment of the specific time of onset for each patient with intracerebral hemorrhage.

Finally, all patients in this study were Chinese, and no other races were included in the study, so the findings may not indicate the actual incidence in other regions. Although the morbidity of patients with nontraumatic ICH is directly due to cerebrovascular rupture, the main causes of ICH are not the same in Western countries as in Asia. Chronic hypertension is a major cause of ICH in China and other Asian countries, but cerebrovascular amyloidosis and oral anticoagulants play a more important role in the occurrence of ICH in Western countries^{3,31–33}. This may be because aging is more severe in Western developed countries, resulting in the deposition of amyloid- β peptide causing degeneration of cerebral vessels and the need for more anticoagulant or antiplatelet drug therapy in the elderly to combat the occurrence of ischemic diseases³⁴. Hypertension can lead to massive expression of vascular extracellular matrix such as laminin and fibronectin, which will destroy the structure of cerebrovascular, leading to vascular sclerosis as well as increased permeability^{35,36}. This is also the reason why cerebral hemorrhage shows a strong association with hypertensive disorders³⁷. In China, the incidence of hypertension is 2.5 times higher than that in the United States, and more than 80% of stroke patients have been diagnosed with hypertension^{36,38}. In addition, Chinese patients were more inclined to use a single blood pressure control drug when treating hypertension, and the proportion of polypharmacy combination therapy was only 21.9%, which would result in less effective prevention and control of hypertension^{39,40}. Therefore, the difference in the incidence of hypertension and the difference in medication strategies may be important factors leading to the difference in the causes of ICH between China and Western countries. Future studies using larger samples are needed to support our findings, which will help clinicians find a more rapid and accurate method to judge the occurrence and progression of patients with ICH.

Conclusion

CT irregular shape has an excellent performance in predicting functional outcomes in patients with spontaneous intracerebral hemorrhage. As an imaging marker of NCCT, the irregular shape can help doctors identify patients with rapid disease progression, poor prognosis, and high mortality. Moreover, this is the first study to confirm the statistical significance of D-dimer in predicting irregular shapes and has excellent potential to further explore the pathophysiological mechanism of D-dimer in hematoma enlargement. To improve prediction accuracy and sensitivity, plasma D-dimer level increases can be combined with other cerebral hemorrhage-related factors in subsequent studies.

Data availability

The data that support the findings of this study are available from the corresponding author upon reasonable request.

Code availability

Not applicable.

Received: 13 October 2021; Accepted: 12 May 2022

Published online: 20 May 2022

References

1. Zhao, X. *et al.* Neutrophil polarization by IL-27 as a therapeutic target for intracerebral hemorrhage. *Nat. Commun.* **8**, 602. <https://doi.org/10.1038/s41467-017-00770-7> (2017).
2. Keep, R. F., Hua, Y. & Xi, G. Intracerebral haemorrhage: Mechanisms of injury and therapeutic targets. *Lancet Neurol.* **11**, 720–731. [https://doi.org/10.1016/s1474-4422\(12\)70104-7](https://doi.org/10.1016/s1474-4422(12)70104-7) (2012).
3. Qureshi, A. I., Mendelow, A. D. & Hanley, D. F. Intracerebral haemorrhage. *Lancet* **373**, 1632–1644. [https://doi.org/10.1016/s0140-6736\(09\)60371-8](https://doi.org/10.1016/s0140-6736(09)60371-8) (2009).

4. Davis, S. M. *et al.* Hematoma growth is a determinant of mortality and poor outcome after intracerebral hemorrhage. *Neurology* **66**, 1175–1181. <https://doi.org/10.1212/01.wnl.0000208408.98482.99> (2006).
5. Takeda, R. *et al.* A practical prediction model for early hematoma expansion in spontaneous deep ganglionic intracerebral hemorrhage. *Clin. Neurol. Neurosurg.* **115**, 1028–1031. <https://doi.org/10.1016/j.clineuro.2012.10.016> (2013).
6. Yu, Z. *et al.* Comparison of hematoma density heterogeneity and ultraearly hematoma growth in predicting hematoma expansion in patients with spontaneous intracerebral hemorrhage. *J. Neurol. Sci.* **379**, 44–48. <https://doi.org/10.1016/j.jns.2017.05.049> (2017).
7. Demchuk, A. M. *et al.* Prediction of haematoma growth and outcome in patients with intracerebral haemorrhage using the CT-angiography spot sign (PREDICT): A prospective observational study. *Lancet Neurol.* **11**, 307–314. [https://doi.org/10.1016/S1474-4422\(12\)70038-8](https://doi.org/10.1016/S1474-4422(12)70038-8) (2012).
8. Kanj, A. *et al.* From spot sign to bleeding on the spot: Classic and original signs of expanding primary spontaneous intracerebral hematoma. *Case Rep. Radiol.* **2021**, 9716952. <https://doi.org/10.1155/2021/9716952> (2021).
9. Han, J. H., Lee, J. M., Koh, E. J. & Choi, H. Y. The spot sign predicts hematoma expansion, outcome, and mortality in patients with primary intracerebral hemorrhage. *J. Korean Neurosurg. Soc.* **56**, 303–309. <https://doi.org/10.3340/jkns.2014.56.4.303> (2014).
10. Boulouis, G., Morotti, A., Charidimou, A., Dowlatshahi, D. & Goldstein, J. N. Noncontrast computed tomography markers of intracerebral hemorrhage expansion. *Stroke* **48**, 1120–1125. <https://doi.org/10.1161/strokeaha.116.015062> (2017).
11. Morotti, A., Arba, F., Boulouis, G. & Charidimou, A. Noncontrast CT markers of intracerebral hemorrhage expansion and poor outcome: A meta-analysis. *Neurology* **95**, 632–643. <https://doi.org/10.1212/WNL.0000000000010660> (2020).
12. Zhou, Q. *et al.* Plasma D-dimer predicts poor outcome and mortality after spontaneous intracerebral hemorrhage. *Brain Behav.* **11**, 462–468. <https://doi.org/10.1002/brb3.1946> (2021).
13. Morotti, A. *et al.* Association between serum calcium level and extent of bleeding in patients with intracerebral hemorrhage. *JAMA Neurol.* **73**, 1285–1290. <https://doi.org/10.1001/jamaneurol.2016.2252> (2016).
14. Morotti, A. *et al.* Standards for detecting, interpreting, and reporting noncontrast computed tomographic markers of intracerebral hemorrhage expansion. *Ann. Neurol.* **86**, 480–492. <https://doi.org/10.1002/ana.25563> (2019).
15. Wada, R. *et al.* CT angiography “spot sign” predicts hematoma expansion in acute intracerebral hemorrhage. *Stroke* **38**, 1257–1262. <https://doi.org/10.1161/01.STR.0000259633.59404.f3> (2007).
16. Goldstein, J. N. *et al.* Contrast extravasation on CT angiography predicts hematoma expansion in intracerebral hemorrhage. *Neurology* **68**, 889–894. <https://doi.org/10.1212/01.wnl.0000257087.22852.21> (2007).
17. Sporns, P. B. *et al.* Comparison of spot sign, blend sign and black hole sign for outcome prediction in patients with intracerebral hemorrhage. *J. Stroke* **19**, 333–339. <https://doi.org/10.5853/jos.2016.02061> (2017).
18. Li, Q. *et al.* Island sign: An imaging predictor for early hematoma expansion and poor outcome in patients with intracerebral hemorrhage. *Stroke* **48**, 3019–3025. <https://doi.org/10.1161/STROKEAHA.117.017985> (2017).
19. Zhang, M. *et al.* Blend sign is a strong predictor of the extent of early hematoma expansion in spontaneous intracerebral hemorrhage. *Front. Neurol.* **11**, 334. <https://doi.org/10.3389/fneur.2020.00334> (2020).
20. Lin, F. *et al.* Early deterioration and long-term prognosis of patients with intracerebral hemorrhage along with hematoma volume more than 20 ml: Who needs surgery?. *Front. Neurol.* **12**, 789060. <https://doi.org/10.3389/fneur.2021.789060> (2021).
21. Gregson, B. A. *et al.* Individual patient data subgroup meta-analysis of surgery for spontaneous supratentorial intracerebral hemorrhage. *Stroke* **43**, 1496–1504. <https://doi.org/10.1161/strokeaha.111.640284> (2012).
22. Sporns, P. B. *et al.* Triage of 5 noncontrast computed tomography markers and spot sign for outcome prediction after intracerebral hemorrhage. *Stroke* **49**, 2317–2322. <https://doi.org/10.1161/strokeaha.118.021625> (2018).
23. Delcourt, C. *et al.* Hematoma growth and outcomes in intracerebral hemorrhage: The INTERACT1 study. *Neurology* **79**, 314–319. <https://doi.org/10.1212/WNL.0b013e318260cbba> (2012).
24. Morotti, A. *et al.* Predicting intracerebral hemorrhage expansion with noncontrast computed tomography: The BAT score. *Stroke* **49**, 1163–1169. <https://doi.org/10.1161/STROKEAHA.117.020138> (2018).
25. Hu, X. *et al.* Effects of plasma D-dimer levels on early mortality and long-term functional outcome after spontaneous intracerebral hemorrhage. *J. Clin. Neurosci.* **21**, 1364–1367. <https://doi.org/10.1016/j.jocn.2013.11.030> (2014).
26. Chen, C. W. *et al.* Dynamic evolution of D-dimer level in cerebrospinal fluid predicts poor outcome in patients with spontaneous intracerebral hemorrhage combined with intraventricular hemorrhage. *J. Clin. Neurosci.* **29**, 149–154. <https://doi.org/10.1016/j.jocn.2015.10.036> (2016).
27. Sivakumaran, M. & Malton, N. Plasma D-dimer measurement as a predictor of venous thrombosis. *Blood* **102**, 4618. <https://doi.org/10.1182/blood-2003-09-2998> (2003) (author reply 4618–4619).
28. Hua, Y., Keep, R. F., Hoff, J. T. & Xi, G. Brain injury after intracerebral hemorrhage: The role of thrombin and iron. *Stroke* **38**, 759–762. <https://doi.org/10.1161/01.STR.0000247868.97078.10> (2007).
29. Yang, S. *et al.* Effects of thrombin on neurogenesis after intracerebral hemorrhage. *Stroke* **39**, 2079–2084. <https://doi.org/10.1161/STROKEAHA.107.508911> (2008).
30. Brott, T. *et al.* Early hemorrhage growth in patients with intracerebral hemorrhage. *Stroke* **28**, 1–5. <https://doi.org/10.1161/01.str.28.1.1> (1997).
31. Wang, W. *et al.* Prognostic value of ICH score and ICH-GS score in Chinese intracerebral hemorrhage patients: Analysis from the China National Stroke Registry (CNSR). *PLoS ONE* **8**, e77421. <https://doi.org/10.1371/journal.pone.0077421> (2013).
32. Zhao, D. *et al.* Epidemiological transition of stroke in China: Twenty-one-year observational study from the Sino-MONICA-Beijing Project. *Stroke* **39**, 1668–1674. <https://doi.org/10.1161/strokeaha.107.502807> (2008).
33. Toyoda, K. Epidemiology and registry studies of stroke in Japan. *J. Stroke* **15**, 21–26. <https://doi.org/10.5853/jos.2013.15.1.21> (2013).
34. Rosand, J., Hylek, E. M., O'Donnell, H. C. & Greenberg, S. M. Warfarin-associated hemorrhage and cerebral amyloid angiopathy: A genetic and pathologic study. *Neurology* **55**, 947–951. <https://doi.org/10.1212/wnl.55.7.947> (2000).
35. Nag, S. Immunohistochemical localization of extracellular matrix proteins in cerebral vessels in chronic hypertension. *J. Neuro-pathol. Exp. Neurol.* **55**, 381–388. <https://doi.org/10.1097/00005072-199603000-00014> (1996).
36. Lin, X., Wang, H., Rong, X., Huang, R. & Peng, Y. Exploring stroke risk and prevention in China: Insights from an outlier. *Aging* **13**, 15659–15673. <https://doi.org/10.18632/aging.203096> (2021).
37. O'Donnell, M. J. *et al.* Global and regional effects of potentially modifiable risk factors associated with acute stroke in 32 countries (INTERSTROKE): A case–control study. *Lancet* **388**, 761–775. [https://doi.org/10.1016/S0140-6736\(16\)30506-2](https://doi.org/10.1016/S0140-6736(16)30506-2) (2016).
38. Lu, Y. *et al.* Comparison of prevalence, awareness, treatment, and control of cardiovascular risk factors in china and the United States. *J. Am. Heart Assoc.* <https://doi.org/10.1161/jaha.117.007462> (2018).
39. Lu, J. *et al.* Prevalence, awareness, treatment, and control of hypertension in China: Data from 1.7 million adults in a population-based screening study (China PEACE Million Persons Project). *Lancet* **390**, 2549–2558. [https://doi.org/10.1016/S0140-6736\(17\)32478-9](https://doi.org/10.1016/S0140-6736(17)32478-9) (2017).
40. Gu, Q., Burt, V. L., Dillon, C. F. & Yoon, S. Trends in antihypertensive medication use and blood pressure control among United States adults with hypertension: The National Health And Nutrition Examination Survey, 2001 to 2010. *Circulation* **126**, 2105–2114. <https://doi.org/10.1161/circulationaha.112.096156> (2012).

Acknowledgements

This work was supported by the National Natural Science Foundations of China (81971135); Natural Science Foundations of Heilongjiang (YQ2020H014); the “Chunhui Plan” of the Ministry of Education (HLJ2019009); Distinguished Young Foundations of the First Affiliated Hospital of Harbin Medical University (HYD2020JQ0014).

Author contributions

Substantial contributions to the conception or design of the work: C.L., H.Z., L.W. and G.Y. Substantial contributions to the acquisition, analysis, or interpretation of data for the work: Q.J., E.L., C.Y., Y.L., Z.S., H.X., X.X., J.S., B.F., and B.Z. Drafted the work: C.L., G.Y., H.Z., L.W., and B.Z. Revised the manuscript critically for important intellectual content: all authors. Final approval of the version to be published: all authors. Agreement to be accountable for all aspects of the work in ensuring that questions related to the accuracy or integrity of any part of the work are appropriately investigated and resolved: D.Z., X.C., N.W., L.W., and G.Y.

Competing interests

The authors declare no competing interests.

Additional information

Supplementary Information The online version contains supplementary material available at <https://doi.org/10.1038/s41598-022-12536-3>.

Correspondence and requests for materials should be addressed to N.W., L.W. or G.Y.

Reprints and permissions information is available at www.nature.com/reprints.

Publisher’s note Springer Nature remains neutral with regard to jurisdictional claims in published maps and institutional affiliations.



Open Access This article is licensed under a Creative Commons Attribution 4.0 International License, which permits use, sharing, adaptation, distribution and reproduction in any medium or format, as long as you give appropriate credit to the original author(s) and the source, provide a link to the Creative Commons licence, and indicate if changes were made. The images or other third party material in this article are included in the article’s Creative Commons licence, unless indicated otherwise in a credit line to the material. If material is not included in the article’s Creative Commons licence and your intended use is not permitted by statutory regulation or exceeds the permitted use, you will need to obtain permission directly from the copyright holder. To view a copy of this licence, visit <http://creativecommons.org/licenses/by/4.0/>.

© The Author(s) 2022